Seasonal hydrogen storage decisions under constrained electricity distribution capacity

Fokkema, Jan Eise; uit het Broek, Michiel A.J.; Schrotenboer, Albert H.; Land, Martin J.; van Foreest, Nicky D.

Published in:
Renewable Energy

DOI:
10.1016/j.renene.2022.05.170

Renewable Energy 195 (2022) 76–91

Contents lists available at ScienceDirect

Renewable Energy

journal homepage: www.elsevier.com/locate/renene

Seasonal hydrogen storage decisions under constrained electricity distribution capacity

Jan Eise Fokkema [a, *], Michiel A.J. uit het Broek [a], Albert H. Schrotenboer [b], Martin J. Land [a], Nicky D. Van Foreest [a]

[a] Department of Operations, University of Groningen, PO Box 800, 9700 AV, Groningen, the Netherlands
[b] Department of Industrial Engineering and Innovation Sciences, Eindhoven University of Technology, PO Box 513, 5600 MB, Eindhoven, the Netherlands

ARTICLE INFO

Article history:
Received 24 February 2022
Received in revised form
19 May 2022
Accepted 31 May 2022
Available online 7 June 2022

Keywords:
Renewable energy
Hydrogen storage
Decentralized power generation
Grid congestion
Inventory control
Markov decision process

ABSTRACT

We consider a profit-maximizing renewable energy producer operating in a rural area with limited electricity distribution capacity to the grid. While maximizing profits, the energy producer is responsible for the electricity supply of a local community that aims to be self-sufficient. Energy storage is required to deal with the energy productions' uncertain and intermittent character. A promising, new solution is to use strategic hydrogen reserves. This provides a long-term storage option to deal with seasonal mismatches in energy production and the local community's demand. Using a Markov decision process, we provide a model that determines optimal daily decisions on how much energy to store as hydrogen and buy or sell from the power grid. We explicitly consider the seasonality and uncertainty of production, demand, and electricity prices. We show that ignoring seasonal demand and production patterns is suboptimal and that introducing hydrogen storage transforms loss-making operations into profitable ones. Extensive numerical experiments show that the distribution capacity should not be too small to prevent local grid congestion. A higher storage capacity increases the number of buying actions from the grid, thereby causing more congestion, which is problematic for the grid operator. We conclude that a profit-maximizing hydrogen storage operation alone is not an alternative to grid expansion to solve congestion, which is essential knowledge for policy-makers and grid operators.

1. Introduction

Renewable energy sources have become increasingly popular. For example, renewable energy production in the EU has increased from 9.6% in 2004 to 18.9% in 2018 [14]. However, seasonality mismatches between supply and demand are among the main challenges that should be dealt with to facilitate growth in renewable energy production. Large solar parks tend to be located in rural areas where land is relatively cheap, even though the electricity grid infrastructure is often limited. This typically causes cable congestion at the location where the solar park is connected to the grid, which causes outages, grid balance problems, and affects operational costs of the electricity grid [29,47]. The high peaks of solar energy production in summer often cause cable congestion, which may inhibit the installation of new solar parks. For the grid operator, designing electricity grids that can accommodate location-specific energy generation and do consider physical constraints is a challenging task [33].

Connecting hydrogen storage to solar parks is a promising method to spread the feed-in to the electricity grid throughout the year, thereby mitigating cable congestion in the summer [1]. It is also suitable as a long-term and strategic buffer to alleviate seasonal mismatches in production and local electricity demand.

Owners of solar parks with hydrogen storage (SPH) facilities connected to an external electricity grid face variable electricity prices as a result of market mechanisms to balance the grid, match supply and demand, and reduce congestion. For example, location-specific (nodal) electricity prices are a solution to reduce grid congestion caused by renewable energy sources [37]. Furthermore, time-of-use tariffs are expected to become more common since these provide advantages to grid operators in alleviating expected congestion [43]. The resulting market mechanisms facilitate the redispatching of energy production by stimulating additional

* Corresponding author. Nettelbosje 2, 9747 AE, Groningen, the Netherlands.
E-mail addresses: j.e.fokkema@rug.nl (J.E. Fokkema), michieluithetbroek@gmail.com (M.A.J. uit het Broek), a.h.schrotenboer@tue.nl (A.H. Schrotenboer), m.j.land@rug.nl (M.J. Land), n.d.foreest@rug.nl (N.D. Van Foreest).

https://doi.org/10.1016/j.renene.2022.05.170

production in areas without congestion and reducing production in areas of congestion by using nodal or zonal prices [50]. Electricity prices are also determined by other factors such as congestion in other areas of the grid, the balancing market, and supply and demand at the national level. As a result, facility owners' electricity prices are stochastic and uncertain. This requires SPH facility owners to take into account these stochastic prices to maximize their profits.

Electricity generated by solar parks directly supplies a local electricity demand of connected households in a rural area. Excess-produced electricity can also be fed to the electricity grid or stored in a nearby hydrogen storage location. The local consumption of the generated electricity avoids energy-transportation over long distances. It enables fulfilling a local electricity demand of households who require a stable supply of green electricity and desire to be self-sufficient. The electricity demand of consumers and solar energy production is characterized by differences in seasonality [2,6]. The confinement of the produced energy in the area of generation, seasonality differences in supply and local demand, and variable electricity prices have significant consequences for the facility owner's decision to store energy and the resulting congestion levels at the cable connection observed by the grid operator. Efficient long-term strategies that determine when energy is stored as hydrogen and sold to or bought from the electricity grid are vital in achieving successful renewable energy penetration. Since hydrogen storage is characterized by relatively high investment costs and limited conversion efficiencies, these strategies become even more critical in enhancing the economic viability of hydrogen storage.

This paper focuses on a profit-maximizing SPH facility that faces daily decisions on how much hydrogen to store, how much electricity to buy from and sell to the grid while providing a local electricity demand of connected households with a stable supply of green electricity.

While our primary focus is on the SPH facility owner, we also investigate the congestion levels at the cable connection from the grid operator's perspective due to the SPH owner's profit-maximizing decisions. The decision to store energy by the SPH facility owner is affected by the presence of seasonality in supply and demand. It is also dependent on the level of solar energy production, the amount of local electricity demand, the amount of hydrogen in storage, and the current electricity price. Additionally, solar energy production levels, electricity demand, and prices in the future are uncertain. For example, even though solar energy production can be predicted rather accurately for several days in advance, specific days' solar energy production levels are uncertain when predicted for more extended periods, such as months. As a result of seasonal patterns, solar energy production and electricity demand's stochastic behavior is time-dependent. These aspects affect storage decisions throughout the year. A Markov decision process formulation is proposed to obtain optimal policies for the above problem. Although we take daily aggregated decisions that ignore intra-day fluctuations, it does not affect our long-term strategic focus for which hydrogen storage is most suitable. Namely, inspired by practice, we assume that a battery handles the intra-day fluctuations so that, from a technical perspective, the electrolyzer is provided with stable loads to maximize its conversion efficiency. Using a battery to balance load of the electrolyzer facilitates the utilization of the electrolyzer. For example [36], found that using a battery to balance the load of the electrolyzer enabled larger utilization rates by providing a stable load. This can also be attributed to the fact that a battery enables the electrolyzer to be used during the day at times when there is no PV production [31].

We make the following contributions. Firstly, we identify the characteristics of optimal storage policies for solar field operators with hydrogen storage. These policies differ from short-term battery storage policies due to seasonality effects, annual timescales, and hydrogen storage for long-term and strategic energy storage. The policy characteristics include price thresholds for each period which depend on the inventory level, price, and net production after demand. Secondly, we show how the facility owner's profit-maximizing decisions either solves or creates congestion problems for the grid operator, which occur at the cable to which the solar park is connected. This results from selling or buying-related decisions depending on the cable distribution capacity and includes the actions taken during overages and shortages throughout the year. Thirdly, we indicate how different combinations of storage and distribution capacity affect these decisions. Next, we analyze profits, congestion levels, and electrolyzer utilization by highlighting the trade-off between profits for the facility owner and congestion levels for the grid operator. Finally, we show how conversion losses and differences between selling and buying prices affect these results.

The remainder of this paper is organized as follows. A literature review is presented in Section 2. Section 3 describes the problem and Section 4 formulates a model. Section 5 provides an overview of the calibration of the parameter settings and the base case system that we consider. Section 6 provides a sensitivity analysis of key performance indicators based on the parameter settings of each of the system elements' capacities. Section 7 provides concluding remarks.

2. Literature review

The existing literature has mostly addressed energy management strategies in which the owner of an energy storage device decides when to buy or sell energy from or to the grid. For a detailed review of energy management decisions for electric storage systems, we refer to Weitzel and Glock [51] and Zakaria et al. [54]. While seasonality differences between supply and demand are important characteristics of renewable energy systems, most papers focus on intraday and day-ahead buying and selling decisions using battery storage for short planning horizons and small discretization levels. In contrast, our approach focuses on hydrogen storage decisions for longer planning horizons covering seasonality during a year. We take into account limited electricity grid distribution capacity that supports the need for local storage. Seasonal patterns in supply and demand, limited grid infrastructure, and electrolyzer and fuel-cell constraints all affect storage decisions.

The literature on energy management decisions optimizes grid interactions using storage by treating supply levels as deterministic [11,38,55] or by optimizing the buying, selling, or storage decisions in which the uncertainty of the generated renewable energy is taken into account [17–20,23,24,26,42,48]. Literature on energy procurement decisions without storage include Wang and Deng [49] and Woo et al. [52]. For example, Wang and Deng [49] analyze an energy procurement problem for a centralized energy aggregator that can control both procurement and consumption within a 24-h planning horizon in which wind energy is generated. From the perspective of a grid distribution operator, Woo et al. [52] address the energy procurement decisions of a grid distributor that need to balance procurement risks and expected costs. Regarding prices, Densing [10], Hassler [20], Jiang and Powell [23,24], Zhou et al. [56] specifically take into account stochastic electricity prices, whereas Grillo et al. [18], Keerthisinghe et al. [26], Shin et al. [42], Steffen and Weber [46] treat these as deterministic. These studies are explained in more detail below.

Several studies that consider hydrogen systems connected to solar or wind power and the electricity grid have developed buying or selling policies that either take into account electricity prices that are known beforehand or use a heuristic approach. For example, Hemmati et al. [21] consider the interactions with the electricity grid using a hybrid storage system with a battery, a hydrogen storage facility with a fuel cell and use fixed hourly prices. Rouholamini and Mohammadian [41] consider the energy management of a hydrogen storage tank connected to wind and solar power, an electrolyzer and the electricity grid by using heuristic policies. Moreover, Bernal-Agustín and Dufo-López [4] examine the production of hydrogen for use in vehicles, and surplus electricity that is sold to the grid with a fixed price.

Studies that jointly optimize the use of storage and the decision to buy from or sell to the grid mostly focus on detailed intra-day decisions [17–20,23,24,26,42]. For example, Jiang and Powell [24] address the arbitrage problem with energy storage to place bids in an hour-ahead spot market. Grillo et al. [18] optimally schedule batteries with renewable energy. Gönsch and Hassler [17], Hassler [20] optimize energy arbitrage decisions for short time horizons within one day and time intervals of 15 min. Keerthisinghe et al. [26] develop energy-storing policies for a battery in a residential home within single days. In contrast, Shin et al. [42] have addressed the problem for both intraday and yearly planning horizons. Zhou et al. [56] address the energy storage arbitrage problem within a week for 5-min periods. They address seasonality by using specific parameter settings for each week that is solved. While these papers all address detailed arbitrage and storing decisions for short time horizons using batteries, hydrogen or a combination, none of them provide an integrated approach to address the issue of seasonality over one year.

The related literature on energy storage and arbitrage that has included transmission or distribution capacity constraints is relatively scarce. Larscheid et al. [30] examine the use of electrolyzers to counteract grid congestion and maximize revenues by buying from the electricity grid and perform cross-commodity trading by selling hydrogen. Fertig and Apt [15] investigate the economics of pairing a wind farm with compressed air energy storage and limited transmission capacity. They use heuristic control policies to decide on buying and selling to the grid. Most work that incorporates transmission constraints focuses on energy storage planning from a strategic perspective rather than an operational perspective. For example, Babrowski et al. [3] optimize storage planning for the German electricity sector while including transmission constraints. Wang et al. [50] examine to what extent transmission congestion affects the profitability of arbitrage by energy storage, including transmission constraints. Jorgenson et al. [25] analyze to what extent transmission or storage can assist in reducing curtailment. Korpås and Greiner [27] consider transmission constraints, by connecting an electrolyzer to weak power grids and using hydrogen as a load management method.

To the best of our knowledge, Zhou et al. [56] and Gönsch and Hassler [17] are the only papers that have included transmission constraints in focusing on the operational decision of when to buy, sell or store energy, while taking into account stochastic electricity prices. They have addressed wind-based electricity with co-located storage. However, their numerical study encompasses only one week and does not consider hydrogen storage, which would become relevant for longer terms. To the best of our knowledge, optimal buying and selling policies for uncertain and seasonal electricity production, local electricity demand and price levels have not yet been considered for solar field operators with hydrogen storage, even though this is important for the economic viability of hydrogen storage facilities. Moreover, the effect of these policies on the interactions with the electricity grid connection throughout the year have not yet been examined, even though this is essential knowledge for grid operators.

3. Problem description

We consider a profit-maximizing renewable energy producer using a photovoltaic (PV) system (i.e., solar panels) who is also the owner of a hydrogen storage facility and provides the energy to a local electricity demand. For instance, it may form a self-sufficient community together with a small village, by selling the energy to an energy company for a fixed price c^d, which in turn provides the energy to the directly-connected households. The energy producer can also sell or buy electricity from the electricity grid, and the co-located hydrogen storage is used to store electricity in the form of hydrogen temporarily. We consider a time horizon $\mathcal{T}$ that resembles a complete year, and each period $t \in \mathcal{T}$ resembles a single day. Fig. 1 provides a graphical overview of the considered system [16]. The left side of Fig. 1 shows the solar energy producer and the hydrogen storage facility, and the right side shows the local electricity demand and electricity grid connection. Our goal is to decide upon when and how much to 1) sell and buy electricity from the grid, 2) store or consume hydrogen from our local storage to satisfy local demand and maximize profits. We assume the owner of the storage and PV facilities and the households are connected to the grid through an external connection and are the single users of this connection.

In the following, we describe our system in detail. Table 1 provides an overview of all the parameters and variables.

The installed capacity of solar energy production in MWp is assumed constant throughout the year and denoted by w. Solar energy production per day is a random variable Y_t, where the dependency on the period follows from seasonal differences in energy production throughout the year. Local electricity demand is denoted by the random variable D_t and is normally distributed with mean μ_t and a period-independent standard deviation σ. As it is optimal to satisfy local demand with local supply of solar energy (this comes at no cost), we assume that the produced electricity Y_t is first used to supply and sell it to the local demand D_t with a constant and fixed price c^d. We then convert our production and demand process in a net solar energy production level $\bar{Y}_t = Y_t - D_t$. The net solar energy production per day $\bar{Y}_t$ can then be modeled via a truncated probability distribution $f^{\bar{y}}(t)$ with a maximum of l_t^+ in period t due to a restricted installed capacity of solar energy.

Hydrogen inventory x_t is held inside a hydrogen storage tank with energy capacity m. The tank is filled using an electrolyzer with a maximum rate k^+ at which energy can be stored per period and a conversion efficiency of α where $\alpha \leq 1$. Moreover, the producer can

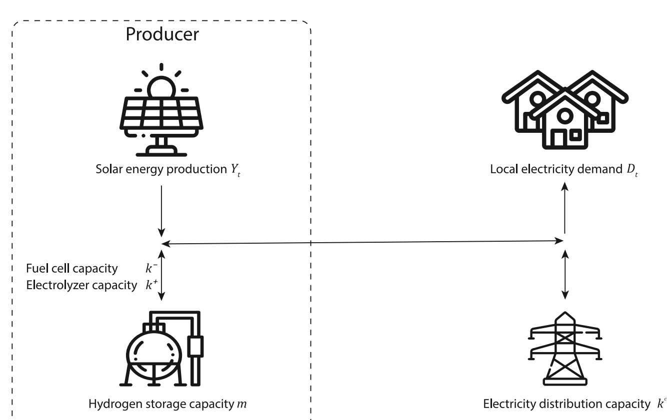

Fig. 1. Visual representation of the studied system.

Table 1
Sets, parameters and state variables.

Sets	
$\mathcal{T}$	Set on the number of periods $\mathcal{T} = \{0, \ldots, T\}$
Parameters	
w	Installed peak capacity of the solar park (MWp)
l_t^+	Maximum amount of solar energy that can be generated (MWh) in period t
m	Maximum hydrogen inventory level (storage capacity, MWh)
k^c	Maximum load sent to the grid per period (distribution capacity, MW)
k^+	Maximum load at which energy can be stored per period (electrolyzer capacity, MWh)
k^-	Maximum load from storage to electricity per period (fuel-cell capacity, MWh)
c	Price markup added to the selling price for buying energy from the grid
c^d	Price for selling energy to the connected local demand (MWh)
α	Conversion efficiency to storage
s	Penalty per unit of unmet demand
State variables	
$\bar{y}_t$	Net production realization after demand (MWh) in period t
c_t	Prevailing selling price of electricity in period t
x_t	Inventory level (MWh) in period t
Stochastic variables	
Y_t	Solar energy production in period t
$\bar{Y}_t$	Net production level after demand in period t
C_t	Electricity prices in the local spot market in period t
D_t	Local electricity demand in period t

obtain at most k^- energy units per period from storage due to a limited fuel cell capacity. The grid distribution capacity k^c determines the maximum electricity amount sold to or bought from the grid in each period. Throughout this paper, capacities (except the installed solar energy capacity) are defined as the maximum amount of energy per period that our system's related component can handle.

Electricity prices are stochastic and are modeled as an autoregressive AR(1) process via $C_t = \theta C_{t-1} + \xi_t$, where $\xi_t \sim N(0, \sigma^c)$. Similar to Densing [10] and Zhou et al. [56], we assume that the energy producer is sufficiently small so that it is a price taker that cannot influence electricity prices. Since we explicitly consider long-term strategic decisions, we assume that prices are exogenous, stochastic, and therefore independent of the facility owner's decisions. Since the producer can ramp the feed-in to the grid up and down as a result of price signals, we assume that the prices also reflect the demand for ancillary services on the electricity grid. Consequently, solar energy can be sold to the grid for C_t. The producer can also buy from the grid at a price $C_t + c^+$, where $c^+ \geq 0$ is a fixed price markup which the grid operator imposes to discourage excessive selling to the grid. Similar mechanisms occur in the Netherlands for example, in which annual net production differences sold to the grid are priced at a lower level. As is commonly assumed, it is not possible to simultaneously buy and sell from the grid [see, e.g., 56].

The solar energy producer makes the buying, selling, and storing decisions at the end of each period $t \in \mathcal{T}$. Since hydrogen conversion is associated with relatively high conversion losses and electrolyzers perform better at stable loads, we assume that a battery handles intra-day load fluctuations of net production levels.

The storage owner's objective is to maximize the expected future profits related to interacting with the electricity grid during the planning horizon. The decisions made in each period affect the total profit. These decisions have to satisfy several detailed constraints and depend on the system's state at the end of a period. We discuss these aspects in the next section.

4. Markov Decision Process formulation

We formulate our problem as a Markov decision process (MDP). We first describe our state and action spaces, and the constraints upon them. We also specify our reward function. We then discuss how we discretized our state and action spaces, and formally define our MDP which we solve via backward dynamic programming.

4.1. State and action space

At the end of period t, we observe an inventory level x_t, the current and previous price level c_t and c_{t-1} and net production level after demand $\bar{y}_t$. The price c_{t-1} is included in the state because we consider prices to be an autoregressive process. The transition probability between states also depends on the price level in the previous period. Let $S_t(\bar{y}_t, x_t, c_t, c_{t-1}) \in \mathcal{S}$ be the state of our system in period t. We write $\mathcal{S}$ for the state space. For each state $S_t \in \mathcal{S}$, we define the action $u(S_t) \in \mathbb{R}$ as the number of energy units to buy from or sell to the grid at the end of period t. Negative values represent the number of energy units to buy from the grid.

The action u is bounded by the characteristics of the state S_t. It is most easily described if we consider the range of actions $[-u^{\min}(S_t), u^{\max}(S_t)]$. Here, $u^{\min}(S_t) \geq 0$ denotes the maximum amount of energy bought from the grid at the end of a period, and $u^{\max}(S_t) \geq 0$ denotes the maximum amount of energy that can be sold to the grid at the end of a period. In the following, we describe for each state $S_t \in \mathcal{S}$ how to obtain $u^{\min}(S_t)$ and $u^{\max}(S_t)$.

The maximum amount of energy that can be bought $u^{\min}(S_t)$, for all $S_t \in \mathcal{S}$ is the largest value which must satisfy three constraints such that

$$u^{\min}(S_t) \leq k^c \tag{1}$$

$$u^{\min}(S_t) \leq (m - x_t) \Big/ \alpha - \alpha \max\{0, \bar{y}_t\} - \min\{0, \bar{y}_t\} \tag{2}$$

$$u^{\min}(S_t) \leq k^{+} - \max\{0, \bar{y}_t\}. \tag{3}$$

These constraints ensure that the distribution capacity is respected, that we do not store more energy than fits in the storage tank, and that the electrolyzer capacity is respected. The minima and maxima within these constraints ensure correctness in case of net overages and shortages. The maximum amount of energy that can be sold $u^{\max}(S_t)$, for all $S_t \in \mathcal{S}$ is the largest value such that

$$u^{\max}(S_t) \leq k^{c}, \quad u^{\max}(S_t) \leq x_t + \bar{y}_t, \quad u^{\max}(S_t) \leq k^{-}, \tag{4}$$

which indicates that the cable distribution capacity should be respected, that we can sell at most the inventory we have plus the net overage, and that the fuel cell capacity should be respected. Note that these actions allow for unmet demand, in case $\bar{y}_t < 0$. We, therefore, introduce a penalty s per unit of unmet demand that represents a very large negative number to avoid this could happen under any optimal policy. The action space U can then be defined as

$$U = \left\{ \left[-u^{\min}(S_t), u^{\max}(S_t) \right] \middle| S_t \in S, \text{s.t. (1) and (2)}, t \in \mathcal{T} \right\}. \tag{5}$$

the reward $r(u(S_t))$ of taking action $u(S_t)$ is the sum of the revenues and costs during period t as a result of interacting with the grid. It is defined as

$$r(u(S_t)) = u(c_t + \mathbb{1}_{\{u \leq 0\}} c^{+}) + \mathbb{1}_{\{x_{t+1} | u < 0\}} s, \tag{6}$$

where $\mathbb{1}_{(\cdot)}$ equals 1 if $(\cdot)$ evaluates to true, and is 0 otherwise. Here, by slight abuse of notation, we denote by $x_{t+1}|u$ the hypothetical inventory level at time $t+1$ given action $u(S_t)$. If that is negative, demand is unmet and penalty costs s are incurred.

Note that if energy is sent to storage, that is for any state S_t, $-u + \bar{y}_t \geq 0$, the amount of energy that is stored depends on the conversion efficiency α. To avoid numerical issues in the MDP implementation associated with conversion losses for both charging and discharging and resulting fractional numbers, we directly calculate the round-trip conversion losses when sending energy to storage, which is exact.

$$V_n(S_n) = \max_{u(S_n) \in \mathcal{U}} \left\{ r(u(S_n)) + \sum_{\bar{y}_n} \in \bar{\mathcal{Y}}_n \sum_{c_n \in \mathcal{C}} p_{n-1}(\bar{y}_{n-1}, c_{n-1}, c_n) V_{n-1}(S_{n-1}) \right\}. \tag{12}$$

4.2. Discretization

For the numerical analysis, we need to discretize the state space. We discretize the amount of hydrogen inventory, the net production throughout the year, and the observed prices. We define $\mathcal{X}$ as the set of possible net inventory levels, where Δx_t represents the interval size of the inventory levels. The intervals to which an action u belongs are split into equally-sized intervals which correspond to the discretization of the inventory levels Δx_t. We denote the discretized set of actions by $\mathcal{U}$. The stochastic net solar energy production $\bar{Y}_t$ is discretized according to Δj_t, and electricity prices are discretized with Δc_t. Accordingly,

$$\mathcal{X} = \{0, \Delta x_t, 2\Delta x_t, \ldots, m\}, \tag{7}$$

$$\bar{\mathcal{Y}}_t = \{l_t^{-}, \Delta j_t, 2\Delta j_t, \ldots, l_t^{+}\}, \tag{8}$$

$$\mathcal{C} = \{0, \Delta, 2\Delta c_t, \ldots, C\}. \tag{9}$$

4.3. MDP for storing, buying from or selling to the grid

The selling and buying policies result in an inventory process over time in which an immediate reward of $r(u(S_t)))$ is earned after choosing an action at the end of period t. The action is chosen after the solar production and electricity prices have been fully observed at the end of a period. Therefore, the decision-maker knows with certainty to which new inventory level the action will lead in the next period. The future inventory x_{n-1} in period $n-1$ with $n = T - t$ can be defined as.[1]

$$x_{n-1}(u, \bar{y}_n) = x_n + \left\{ \begin{array}{ll} \alpha(u + \bar{y}_n) & \text{if } u + \bar{y}_n \\ \geq 0 u + \bar{y}_n & \text{if } u + \bar{y}_n < 0. \end{array} \right. \tag{10}$$

The transition probability $p_{n-1}(\bar{y}_{n-1}, c_{n-1}, c_n)$ is defined as the probability of net production realization of $\bar{y}_{n-1}$ and a price realization of c_{n-1} in period $n-1$ given price c_n in period n. Similar to Zhou et al. [56], we assume that the underlying stochastic processes are independent. We define $V_0(S_0)$ as the total expected profit at the end of the horizon with $n = 0$ periods to go. We assume that

$$V_0(S_0) = 0. \tag{11}$$

For all other time periods in which $n > 0$, action $u(S_n) \in \mathcal{U}$ can be executed. Accordingly, we define

Via backwards dynamic programming, $V_n(S_n)$ can be obtained for all periods-to-go $n \in \mathcal{T}$. The associated optimal periodic policy $(u_1^*(S_1), u_2^*(S_2), \ldots, u_T^*(S_T))$ that minimizes long-term average rewards is then obtained by iteratively applying backwards dynamic programming upon this system, where $V_0(S_0)$ is calculated according to equation (12) with $V_{n-1}(S_{n-1})$ equal to $V_T(S_T)$ of the previous iteration (equaling zero for the first iteration). Convergence to optimality is proven if all values $V_n(S_n)$ change with the same value (i.e., the long-run average reward) between iterations [39].

[1] For readability, we ignore the case that inventory becomes negative, but this is trivially excluded by taking the maximum of x_{n-1} and 0.

5. Numerical analysis

We start our numerical section by introducing a base-case system for which we provide a detailed numerical analysis (see Section 5.1) and then describe how the price and production processes are fitted (see Section 5.3). We end the section by examining the optimal policy for the base-case system while focusing on the differences between summer and winter. To provide a comparison for the viability of the base-case system, we compare the optimal policy to a system without any hydrogen storage options. A more extensive sensitivity analysis in which all system parameters deviate one-by-one is postponed to Section 6.

5.1. Base-case system

The experiments are based on a planned project of a rural village in the Netherlands in which electricity needs are supplied by a solar park. It comprises a hypothetical solar park with a peak capacity w of 5 MWp that is connected to a local electricity grid in which the connection has a maximum load (k^c) of 30 MWh per day (which corresponds to 1.25 MW). Distribution capacities of 2.5 MW are common in practice for lines that operate at the distribution (local) level rather than the (national) transmission level. In our experiments, we set a more constrained distribution capacity of 1.25 MW, to represent the situation in which the distribution capacity is more constrained. We assume the solar park is connected to a 2.1 MW electrolyzer and a 2.1 MW stack of fuel cells. For both the electrolyzer and fuel cell, this translates to a maximum inflow (k^+) and outflow (k^-) to and from storage of 50 MWh per day. Since only relatively small amounts (up to 16 MWh [5]) can be stored inside a single pressurized vessel, we assume that hydrogen is stored in a co-located large-scale storage location with multiple pressurized vessels (250 bar) with a total capacity of 1000 MWh. Moreover, we assume a round-trip efficiency α of 0.5. This enables avoiding numerical issues and limits the state space of the Markov Decision Process. This number is primarily based on the notion that electrolyzer efficiency may reach up to 76% in the future [22], and PEM electrolyzers which can reach up to 60% when the hydrogen is sufficiently pure [32]. We assume that the satisfied local demand is sold to the households through an energy company with a fixed price of 41.25 per MWh, which is the average of the prices explained in Section 5.3.

5.2. Capital costs

The capital costs of the base case system consists of the solar panels, the electrolyzer, fuel cell system, compression stations, a battery and the hydrogen storage facility.

The 5 MWp installed capacity of solar panels costs 7.5 million EUR, assuming a capital cost of 1.5 EUR/kW [31]. Electrolyzers cost 90 EUR/kW, a 2.1 MW electrolyzer would cost 189,000 EUR. Moreover, with capital cost of 360 EUR/kW, a PEM fuel cell system of 2.1 MW would cost 756,000 [31].

For the hydrogen storage system, we assume the energy is stored in cylinders at a pressure of 250 bar. The total storage in cylinders has a total cost of 18.7 million EUR, assuming a price of 627.99 EUR/kg [53]. We assume compression stations are installed with a sufficient total flow rate of 60 kg/h with a total cost of 600,000 EUR at a cost of 10,000 EUR per kg/hour [53]. Finally, we assume a lithium-ion battery unit is installed of 40 MWh at a cost of 137 EUR/kWh, which amounts to 5.48 million EUR [45].

5.3. Fitting the price, production, and demand process

Day-ahead hourly wholesale electricity prices in euro/MWh in the Netherlands between 2015 and 2019 are obtained from ENTSOE Transparency Platform [12]. These prices are aggregated to daily prices using the intra-day mean. We assume that the electricity prices which apply to the storage owner exhibit similar behavior to wholesale day-ahead electricity prices.

The average daily day-ahead prices exhibited strong autocorrelation (0.872 for a time lag of 1). Moreover, weekly autocorrelation is observed in which autocorrelation is stronger for weekly time intervals than for intra-week intervals. For example, the autocorrelation decreases to 0.773 for lags up to 6 and jumps to 0.815 for lag 7, suggesting that weekday effects are existent. Seasonal effects are not directly apparent from the data.

Inspired by existing approaches in literature (e.g., Ref. [56]), we test three different AR(1) models of the form $C_t = \varphi + \theta C_{t-1} + \xi_t$, where $\xi_t \sim N(0, \sigma^c)$, C_t is the predicted value, C_{t-1} is the observation at $t-1$, φ is a constant, and θ is the AR term with a time lag of 1. First, we fit an AR(1) process to the daily electricity prices in which both monthly and weekday effects are removed from the original observations. Secondly, we fit an AR(1) process to prices in which only weekday effects are removed. Thirdly, we fit an AR(1) process to the original observations. We compare the models by evaluating the standard error of the estimate in relation to the actual observations. The month day and weekday effects are removed similarly as in Ref. [56]. To evaluate the fit of the AR(1) models, the standard error is calculated as $\sqrt{\sum_{t=2}^{T}(C_t - \hat{C}_t)^2/T}$, where T is the number of periods and $\hat{C}_t = \varphi + \theta C_{t-1} + f'(t) + \xi_t$ is the predicted price in period t. The seasonality effects of the electricity prices are described by $f'(t)$ which is defined similarly as in Ref. [56]. For the models in which monthly and weekday effects are removed from the observations, the seasonality function incorporates monthly and weekday effects $f'(t) = \gamma^1 + \gamma^2 \sum_{i=1}^{11} D_t^{2i} + \gamma^3 \sum_{j=1}^{7} D_t^{3j}$, where γ^1 is a constant, and γ^2 and γ^3 are coefficients of dummy variables D_t^{2i} and D_t^{3j} related to monthly and weekly effects respectively. These equal one if day t is in month i or in week j. The coefficients are estimated using linear regression on the actual daily electricity prices. For models 1 and 2, the AR(1) process is fitted to the observations after the seasonality function is subtracted. Because the standard error of the model which is fitted to the original data is the lowest (7.7), as is given in Table 2, it is found to be unnecessary to include the seasonality function. Since the aggregated data also shows no consistency in seasonality effects throughout the 4 years, we do not include month and weekday effects in our AR(1) process.

To model the electricity demand in our base-case system, we assume that the solar park and hydrogen fuel cells connect directly to a set of 1500 houses that are responsible for the local electricity demand. We have obtained data on electricity consumption from the society of the Dutch Energy Data Exchange (NEDU). The data represents average electricity consumption levels per 15 min as a fraction of the total yearly consumption level for 3001 measurements during the years 2016, 2017, and 2018. Since the data is highly aggregated, the data can be scaled to 1500 households to represent our base-case system. We assume that one household on average consumes 2990 kWh in electricity per year [35]. The scaled daily consumption levels, as used in our base-case system, have a minimum of 9.9 MWh, a mean of 12.3 MWh, and a maximum of

Table 2
AR(1) parameters and standard error.

Model	θ	φ	Std. error
1. Remove both month and weekday effects	−0.004	0.89	37.7
2. Remove weekday effects	−0.006	0.91	38.3
3. Fit to original data	5.23	0.87	7.7

16.1 MWh per day.

The data exhibits a strong linear relationship with time in which the average consumption levels follow a V-shape throughout the year. Accordingly, we split the data into two subsets of observations and fit a linear regression to each subset. The splitting procedure is based on minimizing the sum of the standard errors for both models. According to this procedure, model 1 is based on day 1–199, whereas model 2 is based on day 200–365. It is important to note that the splitting procedure is not based on seasonality differences in demand, but on the day that yields the lowest sum of the standard errors for both models. The fitted models are displayed in Table 3. Since the original data is highly aggregated, we assume the data is normally distributed (i.i.d.) with a daily average μ_t and a constant standard deviation σ. Since the standard errors are relatively similar, we chose the highest standard error of both models ($\sigma = 0.62$) as the standard deviation of electricity demand in the experiments. The demand process can be written as $D_t \sim N(\mu_t, \sigma)$.

We assume that the daily solar energy production levels are stochastic. For each day, hourly solar energy production levels between 2005 and 2016 have been obtained from PVGIS [40] and were aggregated to daily amounts. The production levels correspond to an installed capacity of 5 MWp. The original data is aggregated to daily production levels. For each week, the daily observations within the week of 11 years were normalized to a range between 0 and 1 and fitted to a beta distribution to increase the number of observations. Accordingly, daily solar energy production levels are represented by shape parameters for each timer period α_t and β_t. Hence, $Y_t \sim B(\alpha_t, \beta_t)$. Beta distributions are commonly used in modeling daily solar energy production levels [13, 28]. Similar to Boland [6] and Soubdhan et al. [44], we assume that Y_t is independent and identically distributed for each period.

5.4. Optimal policy structure

We solve the MDP associated with the base-case system employing backward dynamic programming. As our states are dependent on the day of the year, we consider 50 years. This is done for numerical certainty, in which this provides the long-term average reward. The results presented correspond to the optimal policy of year 0, and can be interpreted as the policy that maximizes long-term average rewards (see, for a similar approach, Byon and Ding [7]). Implementation is done in C++17 and the MDP is solved on an Intel Xeon 2.5Ghz processor using 4 threads. In the following, we discuss the structure of the optimal policy of the base-case system. The performance of this policy is discussed separately in Section 5.5.

Fig. 2 shows the optimal policies (i.e., the amount of electricity to sell to the grid) for a period in the winter (Period 1) and in the summer (Period 2). For both periods, we present the optimal policies for the first and third quantile of the net production distribution. On the x-axis, we show the observed electricity price and the probability of occurrence. On the y-axis, we portray the inventory level of the hydrogen storage facility. In this way, the four graphs represent a cloudy winter day (top left), a sunny winter day (top right), a cloudy summer day (bottom left), and a sunny summer day (bottom right).

Table 3
Linear models on electricity consumption.

Model	Intercept	Slope	σ
Day 1–199	15.3	−0.0302	0.62
Day 200–365	1.79	0.0372	0.55

From Fig. 2, one can observe four different types of actions that are taken in the optimal policy, in any of the depicted situations. First, if prices are relatively low, the optimal policy prescribes buying as much electricity from the grid as possible. Second, if prices start to increase, it is best to buy or sell the observed net production. Third, dependent on the actual day of the year, it might be optimal to not buy or sell electricity from the grid, as long as enough inventory is on hand. Fourth, if prices are high enough, it is best to sell as much electricity as possible. We observe that the action to not interact with the grid ($u = 0$) takes place for relatively low prices in the summer and high prices in the winter. In the summer, "no interaction" is optimal for relatively low price levels and the net production is then converted to hydrogen. In the winter, net shortages are fulfilled by converting hydrogen to electricity, which also avoids interaction with the grid.

To understand how the optimal policy differs throughout the year, Fig. 3 presents the optimal action as a function of time and the inventory level for the 25% net production percentile and the two price levels ($c_t = 20$ and 60). Fig. 4 does the same for the 75% net production percentile. The action is represented as the resulting change in inventory level.

We observe that the change in inventory has a period-dependent threshold. In the summer (the middle part of both pictures), the inventory at which optimal actions lead to an inventory increase is lower than in the winter, due to oversupply of electricity in the summer and shortages in winter. The inventory levels at which these thresholds occur are similar for both low and high net production levels. Fig. 4 shows that inventory-increasing actions are also prevalent in summer when prices are low (i.e., $c_t = 20$). This indicates the prevalence of seasonal effects in the optimal policies.

This behavior can be attributed to the following dynamics. Early in the year, a higher probability exists of encountering future electricity shortages than later in the year. Therefore, energy is stored at times of low prices early in the year to enable accumulating sufficient inventory for moments of shortages later in the year. Furthermore, buying decisions made early in the year facilitate the potential to benefit from price differences later in the year. These dynamics will be explained in more detail in Section 5.5.

5.5. Optimal policy performance

We simulate the optimal policy of the base-case system for a total of 1,100,000 years, using the first 100,000 years as a warm-up for the simulation. Fig. 5 illustrates the simulation process. Firstly, the optimal policy is calculated using the Markov Decision Process approach described above. Secondly, the model starts a new time period. The demand, the solar production and price level that applies to period t is then sampled from the related distribution. This enables the net production level y_t to be calculated. Finally, the optimal policy u is applied, such that the performance indicators (see below) can be calculated. When the time horizon is reached, the model ends.

Key performance indicators are given in Table 4. As a benchmark, we also provide the statistics of our base-case system if no hydrogen storage is available (BM1), and in case the optimal policy for a yearly average, constant net production (i.e., ignoring seasonal effects) is applied to our base-case system (BM2). Our key performance indicators are mean profits from grid interactions, electrolyzer utilization, and the mean percentage of the time in which congestion occurs at the cable connected to the solar park. Similar to Ref. [9], we define congestion as the event in which the amount of electricity sent to or obtained from the distribution grid equals the distribution capacity to which the supplier or consumer, in this case, the solar park with storage, is connected. Accordingly, the

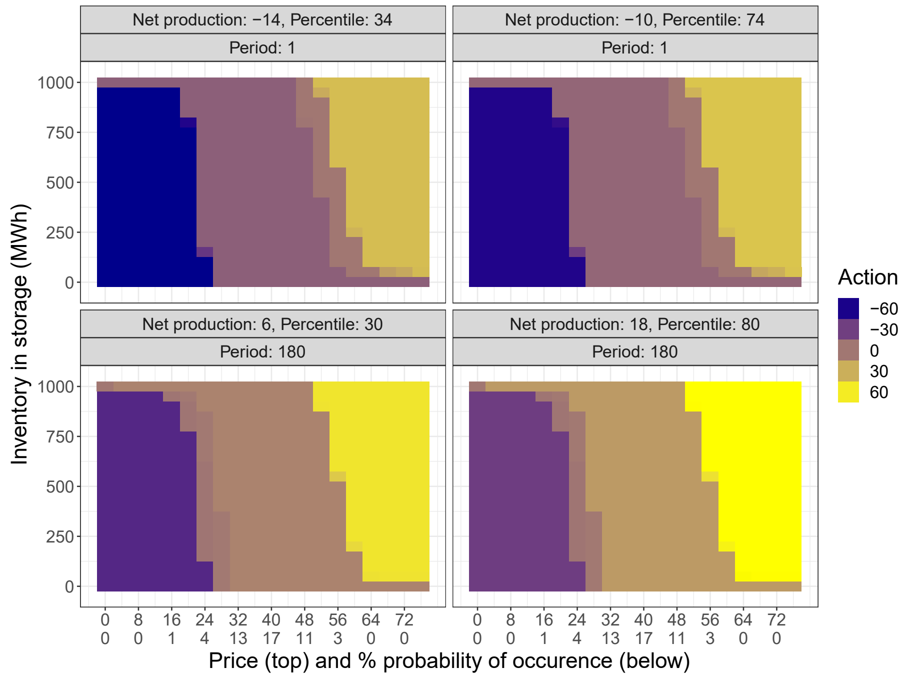

Fig. 2. Optimal policies for winter (top) and summer (below) and for the first (left) and third (right) quantiles of net production.

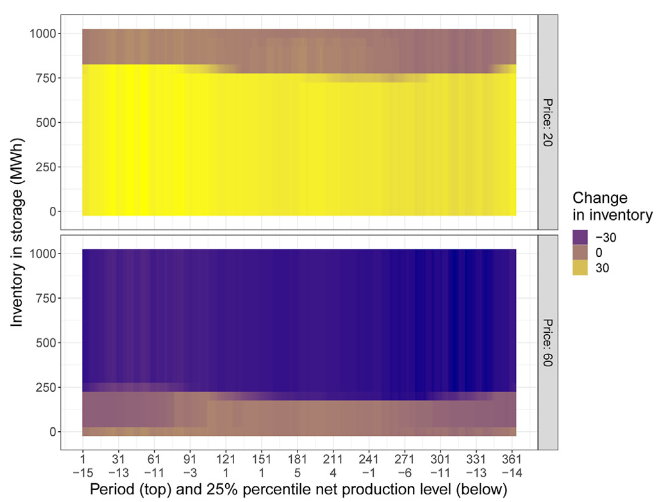

Fig. 3. Optimal policies as the change in inventory (Δx_t) for a low price ($c_t = 20$, top) and high price ($c_t = 60$, below), and a net production percentile of 25%.

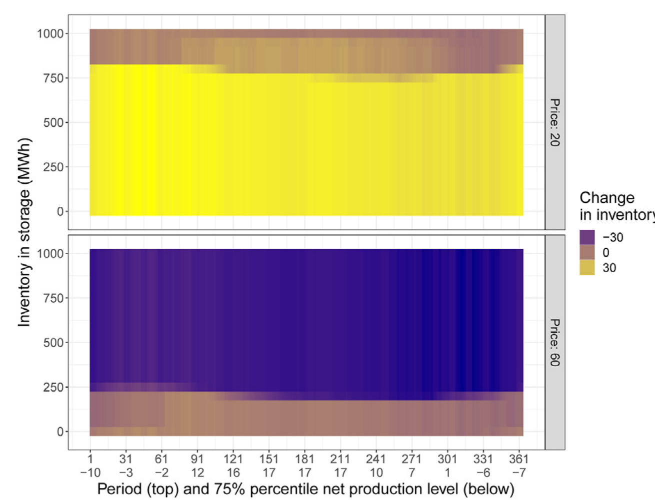

Fig. 4. Optimal policies as the change in inventory (Δx_t) for a low price ($c_t = 20$, top) and high price ($c_t = 60$, below), and a net production percentile of 75%.

mean percentage of time congestion is measured as the mean percentage of time in which selling or buying energy equals the grid distribution capacity. The electrolyzer utilization is given as the percentage use of its full capacity. We also consider the mean revenue from selling energy to local demand at a fixed price of 41.25 per MWh, which is based on the average price considered in our experiments. Finally we calculate the emissions from grid interactions by assuming that every kWh obtained from the grid leads to 0.42 kg of emissions [8].

From Table 4, we observe that adding storage increases mean profit per year from −4060.5 to 6378.5. It is also clear that ignoring seasonality is suboptimal, as the mean profit per year decreases by 3.1% comparing BM2 to the base-case system. The mean electrolyzer utilization denotes the amount of electricity converted to hydrogen given that the electrolyzer is used. It increases 1.8% when we ignore seasonality. The mean percentage of time the cable is used to its full capacity, reflecting situations in which congestion occurs at the cable to which the solar park is connected, equals 8.7% and 8.6% for the base case and when ignoring seasonality (BM2), respectively. Since demand is always met at a fixed price of 41.25 per MWh, the mean revenue from selling to demand remains consistent at 185,046.1. Finally, the mean emissions from grid interactions decrease with 2% when no storage is used compared to the base case system, which can be attributed to reduced buying and selling. Ignoring seasonality reduces emissions with 0.1%.

We further detail the expected fraction of times over all observations in which particular actions are taken throughout the year. In Fig. 6, we detail these actions for a net overage (a) and a net shortage (b). Note, all the actions (i.e., curves) together in (a) and (b)

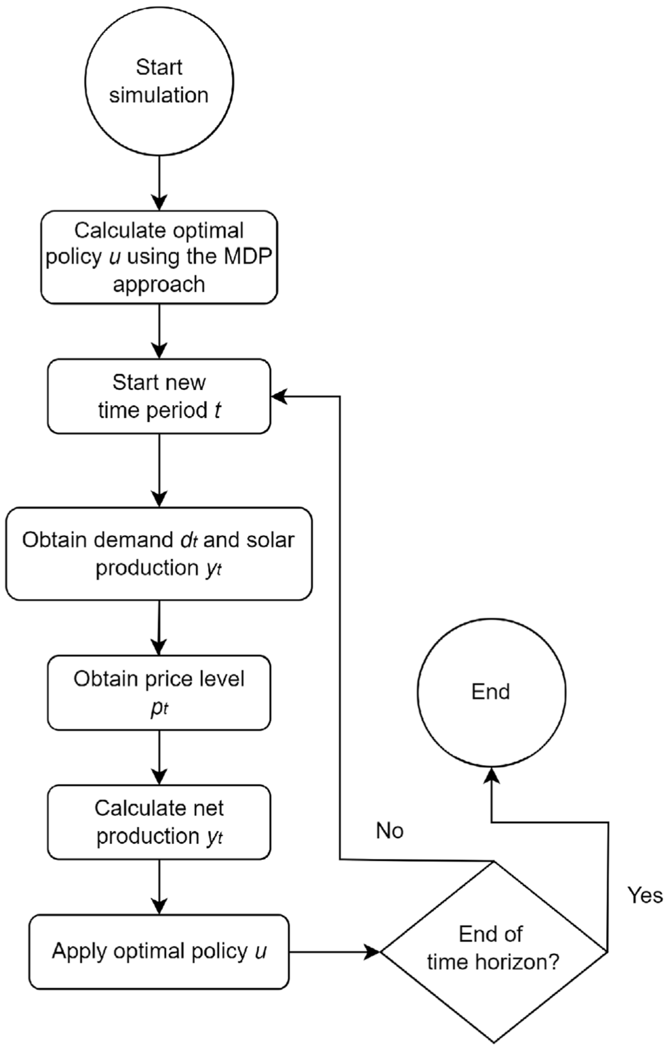

Fig. 5. Flow chart of the simulation process.

sum up to 1.

Given a net shortage, the red points indicate the fraction of times less than the shortage is bought while the remainder is obtained from storage. The green points indicate that more is bought than the shortage while the remainder is stored. The blue points indicate the fraction of times the exact amount of the shortage is bought. The purple points indicate that more inventory is sold than the shortage. Given a net overage, the red points indicate the fraction of times exactly the net overage is sold. The green points indicate the fraction of times the overage is sold plus additional inventory. The blue points indicate the part of the overage that is sold while the remainder is stored. The purple points indicate the fraction of times the overage is stored and additional inventory is bought.

In the case of a net overage for the base-case system, the red points in Fig. 6 (a) show that policies in which exactly the overages are sold to the grid are most prevalent. These follow the seasonality pattern associated with solar electricity production and occur most frequently at 69% of the time in the summer. Policies in which additional electricity is sold out of storage are associated with exploiting price difference possibilities. These are the least common during overages and are highest in summer occurring 5% of the time. Selling less than the overage is also not a common strategy and occurs maximally at 7.7% of the time. This indicates that storage is not used frequently in cases of overages. This also suggests that excess net production can at best be sold directly to the grid to avoid conversion losses when using storage, even at low prices.

For cases of net shortage in Fig. 6 (b), occurrences in which the exact shortage is bought from the grid are most prevalent. The blue points show that the fraction of times the exact amount of the shortage is bought follows an inverse pattern compared to policies in which exactly overages are sold during net overages. These are highest in winter up to 79% and lowest in summer down to 5%. Other policies are very uncommon for the conducted experiments.

Even though these policies are relatively uncommon, the less frequent action types that include not simply selling or buying net production differences, are important for the feasibility of a solar park in rural, possibly congested, areas. For instance, in The Netherlands, it is not allowed to install a solar park with a maximum capacity higher than the distribution capacity, even peaks only occur on clear summer days. The results presented in Fig. 6 indicate that using a storage facility will not interact structurally different from a classic solar park without storage, only its distribution capacity is limited. These are exactly the moments when the less-frequent actions depicted in Fig. 6 play an important role to keep the base-case system feasible. This includes the ability to exploit price differences and to fulfill shortages at times when prices are high. As can be seen in Table 4, a solar park without a storage facility (connected to local electricity demand) yields negative mean profits when demand needs to be solely fulfilled from the electricity grid.

6. Sensitivity analysis

We further investigate the performance of our system, using the key performance indicators already presented in Section 4. We first investigate the impact of changing the distribution capacity (Section 6.1) and afterward discuss the impact of the storage capacity on the performance of the system (Section 6.3). For the distribution and storage capacity, we also provide insights into the interaction with the grid, as this is relevant for future solar park owners and legislators due to its relation to grid congestion issues. We end this section by concisely showing the impact of changing the electrolyzer capacity, conversion efficiency, price mark-up, and production capacity in Sections 6.4-6.7. In each section, we only vary the parameter that is being discussed and set the other parameter values equal to the base-case system.

Table 4
Summary statistics reference case.

KPI	Base-case system	BM1 (no storage)	BM2 (ignoring seasonality)
Mean profit per year from grid interactions	6,378.5	−4,060.5	6,179.3
Mean electrolyzer utilization (%)	21.9	–	22.3
Mean % time congestion (%)	8.7	–	8.6
Mean revenue from selling to local demand	185,046.1	185,046.1	185,046.1
Mean emissions from grid interactions	534,062.1	523,058.3	533,516.1

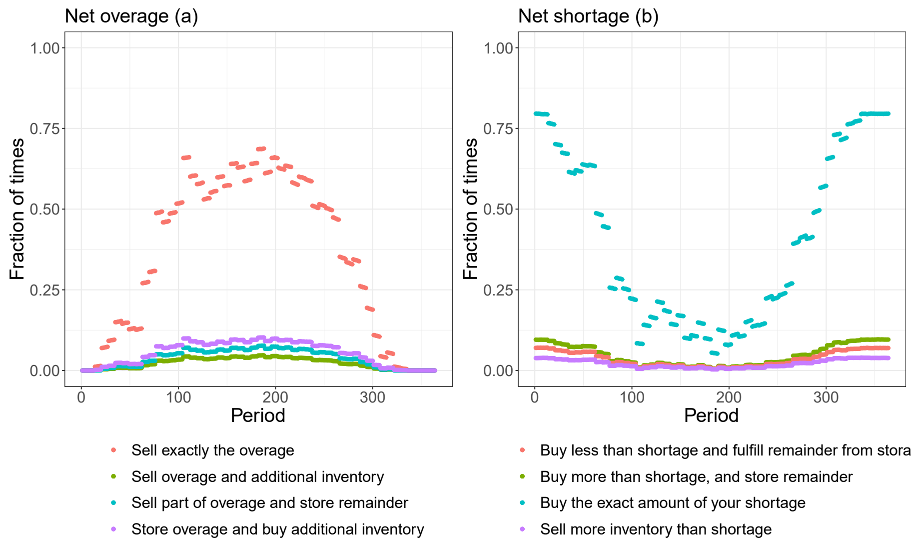

Fig. 6. Fraction of time a certain action occurs over time during a net overage (left) or shortage (right).

6.1. Distribution capacity

We vary the distribution capacity between 1 MWh and 80 MWh per day, which corresponds to 0.04–3.3 MW. In Fig. 7, we see that the mean profit increases for larger distribution capacities, between 4 MWh and 80 MWh per day, because our system becomes less constrained. Distribution capacities below 4 MWh per day are infeasible for our parameter settings, due to unmet demand.

Low distribution capacities up to 10 MWh per day lead to negative profits, which is due to the limited possibility to exploit price differences as local demand should always be satisfied first. For increasing distribution capacities, the electrolyzer utilization increases up to 36.8%. This due to the exploitation of price differences. If prices are low, electricity is bought from the grid to sell it again when prices are high. Finally, the percentage of the time the distribution capacity is fully utilized with congestion at the connected cable approaches 0%, which is expected since the distribution capacity is then only constraining the system for high net production overages.

Fig. 8 (b) (bottom) shows the fraction of times in which the amount of energy bought equals the distribution capacity for different levels of distribution capacity. We label this event as buying-induced congestion that takes place at the connection with the electricity grid. Fig. 8 (a) (top) shows the fraction of times in which sold energy equals the distribution capacity, causing selling-induced congestion.

Fig. 8 shows that relatively low levels of distribution capacity (e.g., $k^c = 5$) cause a combination of buying-induced and selling-induced congestion. This is the result of preventing future shortages and exploiting price difference opportunities. Both types of congestion follow a seasonal pattern. Whereas buying-induced congestion is highest in the winter months, selling-induced congestion is highest in the summer. This can be attributed to net production shortages that occur in the winter and net production overages that occur in the summer. In line with the results in Fig. 6, this indicates that selling net overages and buying net shortages from the grid is a preferred action in general.

When the distribution capacity becomes larger (i.e., $k^c = 10$), more selling-induced congestion occurs since the optimal policy is less impacted by possible shortages in winter. Consequently, less energy is stored and more energy is sold to exploit price differences. Buying-induced congestion simply decreases for higher

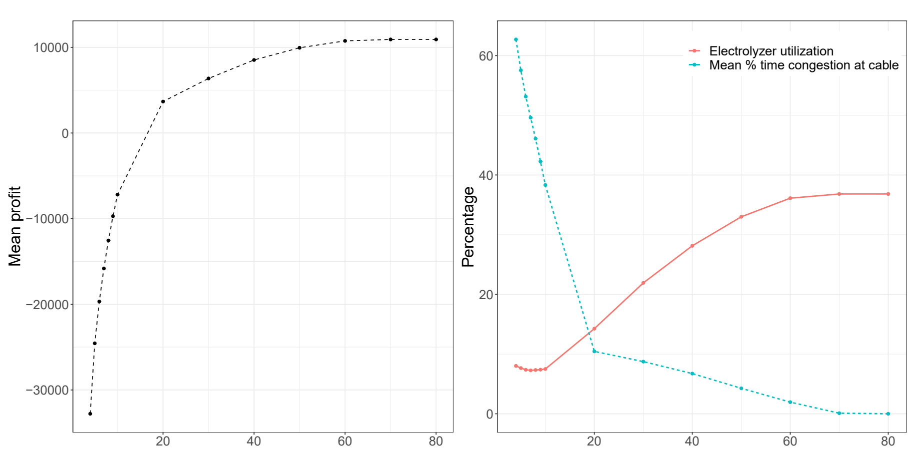

Fig. 7. Summary statistics and distribution capacity (k^c).

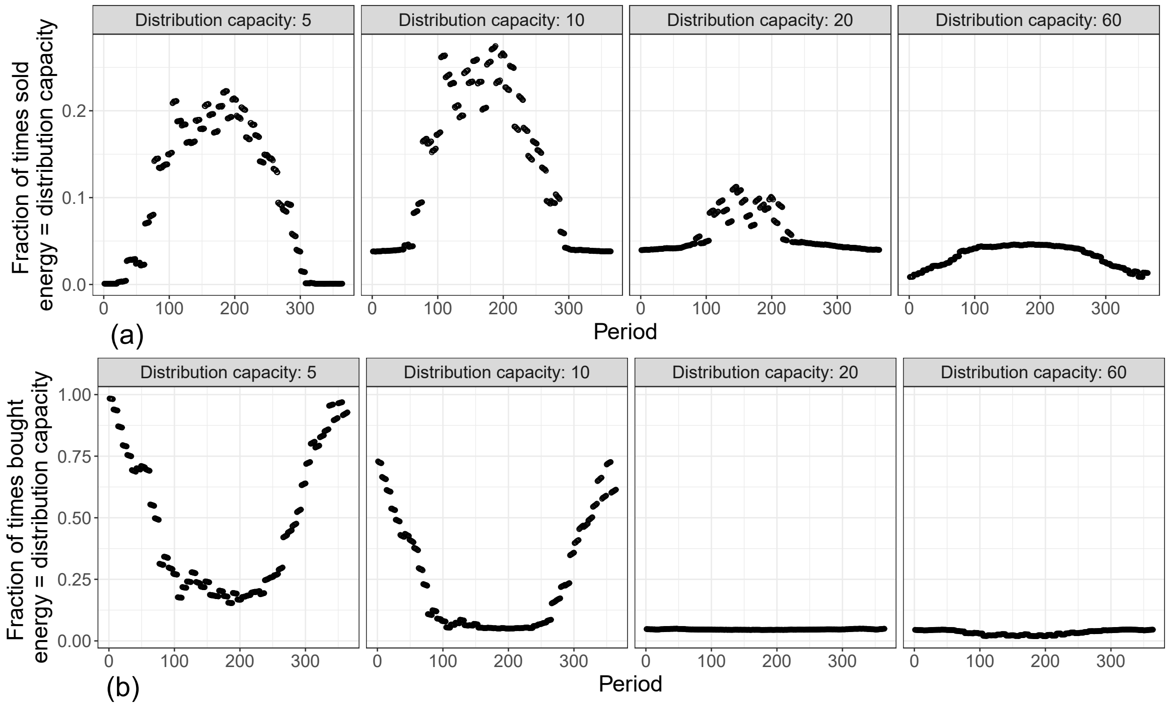

Fig. 8. Fraction of time that sold (a) and bought (b) energy equals the distribution capacity (selling and buying-induced congestion).

distribution capacities as the distribution capacity becomes less-often the limiting factor when net-shortages occur. When capacity increases even more (i.e., $k^c = 20, 60$), the occurrence of both types of congestion decreases, as the net-production realizations can be sold or bought completely from the grid without being restricted by the distribution capacity. Price differences are exploited in higher quantities, while fewer congestion events are observed.

6.2. Capital costs implications

Increasing the distribution capacity from 30 MWh to 60 MWh per day may require an additional 1.25 MW electricity station of 312.500 EUR [34]. Moreover, this requires expanding the cable capacities which cost around 40,000 EUR per kilometer of cable [34]. Depending on the length of the required cables, the capital costs may well exceed 342,500 EUR. For the SPH facility owner, expanding the distribution capacity of 30 MWh to 60 MWh per day leads to a mean profit increase of 4170 EUR per year for the facility owner. This indicates that facility owners benefit from distribution capacity expansions.

6.3. Storage capacity

While the base case used a storage capacity of 1000 MWh and a distribution capacity of 1.25 MW (30 MWh per day), we vary the storage capacity between 100 and 1000 MWh with increments of 100, for three different levels of distribution capacity (10, 40, and 80 MWh per day), see Fig. 9. In this way, we investigate how storage can facilitate congestion reduction when distribution capacity is constrained. Additionally, it allows us to study how profits are affected when distribution capacity is sufficient.

Fig. 9 shows negative mean profits which increase at a marginally decreasing rate with storage capacity for each distribution capacity. For distribution capacity $k^c = 10$ (a), the mean profits are negative due to the highly constrained distribution capacity. Note that storage capacities smaller than 300 MWh are not displayed in Fig. 9 (a). This is because these capacities result in systems where it is not possible to always satisfy local demand. Here, the percentage of unmet demand ranges between 0.005% and 8%, and a penalty for unmet demand is incurred. Electrolyzer utilization levels remain relatively constant (between 6.9% and 7.5%), and congestion levels are not affected by the storage capacity of 300 MWh or higher (the mean percentage time congestion remains between 38.2% and 38.3%). These results indicate that the distribution capacity is too limited across all levels of storage capacities to enable positive profit levels, more effective use of the electrolyzer, and to reduce congestion issues.

Results for $k^c = 40$ and $k^c = 80$ in Fig. 9 (b) and (c) show that congestion issues are not relevant anymore for our distribution capacity. Furthermore, increasing storage capacity to $k^c = 40$ leads to more congestion at the cable connection, due to increasing interactions with the electricity grid. This is in line with the observed electrolyzer utilization for higher storage capacities.

Concluding, hydrogen storage used to supply electricity does not lead to profits when distribution capacity is too constrained and the storage owner aims to maximize profits. While increased levels of distribution capacity reduce peak utilization and the resulting local congestion, seasonal storage does not solve local congestion problems of the grid operator at the connected cable, regardless of the level of installed distribution capacity. To address this, we advise that (1) the grid operator increases distribution capacity and (2) the storage operator should be encouraged to refrain from short-term trading.

6.4. Electrolyzer capacity

We vary electrolyzer capacities k^+ between 2 and 50 MWh per day. Fig. 10 shows that mean profits increase, at a marginally decreasing rate, for increasing electrolyzer capacity. Utilization levels decrease and range between 50% and 29.9% for $k^+ = 2$ to $k^+ = 50$. Profits are positive when the electrolyzer capacity is at

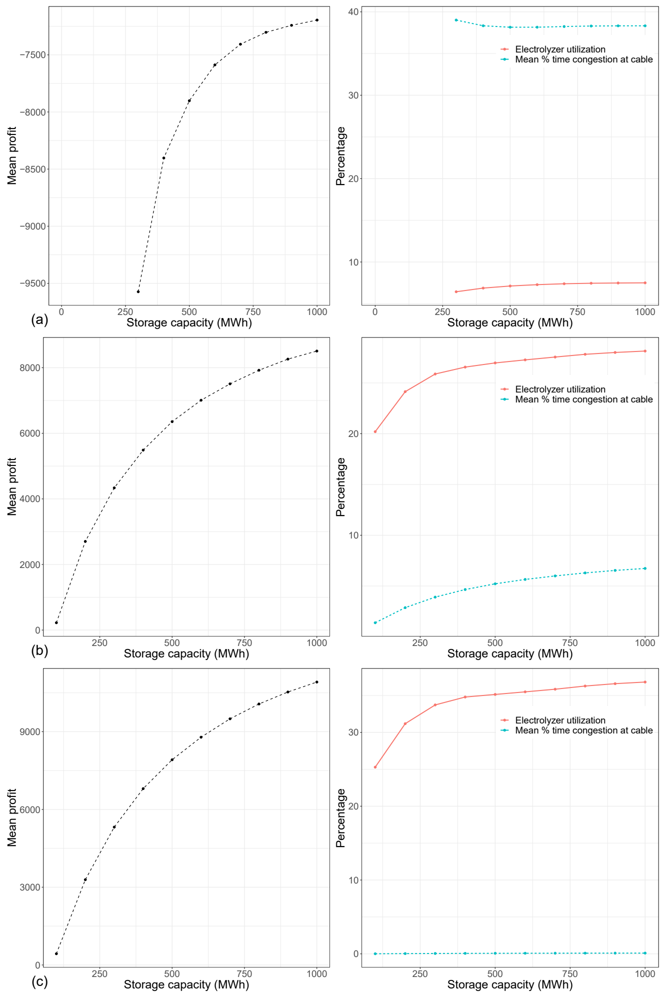

Fig. 9. Summary statistics for varying the storage capacity, for distribution capacities equal to $k^c = 10$ (a), $k^c = 40$ (b) and $k^c = 80$ (c).

least 6 MWh per day (250 kW). Without considering capital expenditures, this suggests that over dimensioning the electrolyzer capacity leads to increased profits, even though utilization levels are reduced. These results suggest that electrolyzer utilization is not a good proxy for profitability as large electrolyzer capacities with a relatively low electrolyzer utilization may lead to more profits than smaller electrolyzer capacities with a relatively high electrolyzer utilization. This only applies to operational profits as capital expenditures are not taken into account.

The mean time in which congestion occurs due to the full utilization of the connected cable increases with higher electrolyzer capacities (up to 50 Mwh per day) and ranges between 0.7 and 8.7%. This can be attributed to the increased trading with the grid. While this enables increased profits for the facility owner, it leads to local congestion for the grid operator. From the perspective of a grid operator, it is, therefore, more beneficial to install a lower-capacity electrolyzer that limits congestion problems when the SPH facility owner aims to maximize profits.

We illustrate the (optimal) actions taken by the facility owner as a result of different electrolyzer capacities. We portray the two combinations of electrolyzer capacities in Fig. 11 ($k^+ = 2$, $k^+ = 10$). It shows the mean fraction of times an action occurs for a net shortage (a) and a net overage (b). The x-axis indicates the period (day) and the y-axis indicates the fraction of time a particular action occurred. The same actions as in Fig. 6 are given.

Given a net shortage and a low electrolyzer capacity (i.e., $k^+ = 2$), the green points in Fig. 11 (a) show that buying the exact amount of the shortage is most prevalent in winter and least prevalent in summer. Other actions are almost non-existent. For a high electrolyzer capacity (i.e., $k^+ = 10$), buying more electricity than the shortage occurs 8% points less frequently on average than for a low electrolyzer capacity (i.e., $k^+ = 2$).

Given a net overage and a low electrolyzer capacity (i.e., $k^+ = 2$), the blue points in Fig. 11 (b) show that actions in which part of the overage is sold and the remainder stored are more prevalent than for high capacity (i.e., $k^+ = 2$), indicating that storing part of an overage is mostly needed for low electrolyzer capacities to cover potential future shortages.

These results indicate that the higher electrolyzer utilization at low capacity (i.e., $k^+ = 2$) is caused by buying and storing additional electricity from the grid in times of shortages or storing in times of overages. The stored energy can be used to cover potential future shortages during times of high prices. When the capacity is higher (i.e., $k^+ = 10$), the risk of supplying future potential shortages from the grid at high prices is reduced, and storing energy is not beneficial.

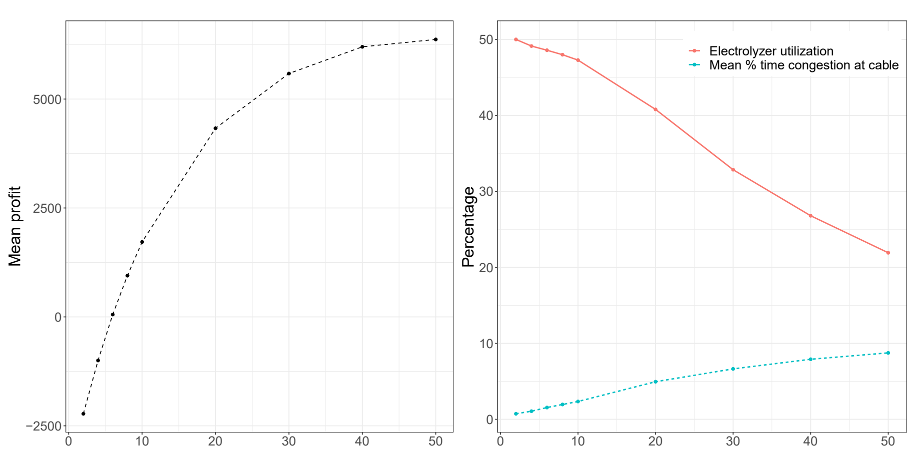

Fig. 10. Summary statistics and electrolyzer capacity (k^+).

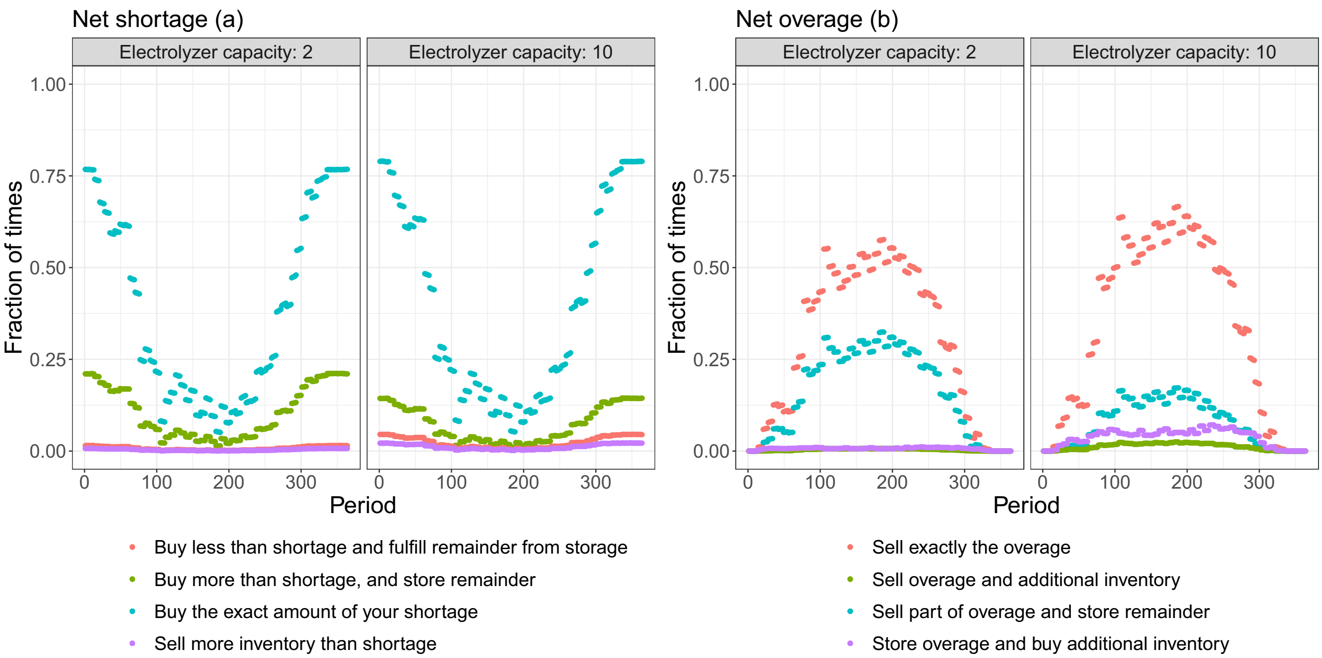

Fig. 11. Fraction of time a certain action occurs over time during a net overage (left) or shortage (right).

6.5. Conversion efficiency

Fig. 12 shows that mean profits are positively related to conversion efficiency since storage becomes increasingly beneficial in both exploiting price differences and covering shortages that do not need to be bought from the grid. For this reason, electrolyzer utilization is also positively related to conversion efficiency. Moreover, congestion at the connected cable increases for higher conversion efficiencies due to a higher frequency of peak loads at the cable connections. This indicates that technological improvements related to hydrogen storage which lead to higher efficiencies also cause increased levels of local congestion at the cable connection.

6.6. Price markup

We vary the price markup that is imposed by the grid operator and is related to buying electricity from the grid (i.e., c^+) between 0 and 5. Fig. 13 illustrates that mean profits are negatively related to the price markup on the buying price. This is expected because price markups on buying electricity discourage the use of storage to benefit from price differences over time. The electrolyzer utilization is reduced from 29% to 22% between price markups of 0 and 5. Reduced grid interaction as a result of higher price markups reduces congestion levels as well. This indicates that the electrolyzer is used less often to buy energy from the grid to benefit from price differentials. This facilitates the use of storage to prevent congestion. This also indicates that price markups are effective as an instrument to the grid operator to reduce congestion levels in which markups can be raised until using storage is not profitable anymore.

6.7. Production capacity

We vary the production capacities of the solar park (i.e., w) between 1 and 10 MWp. Fig. 14 indicates that mean profits appear

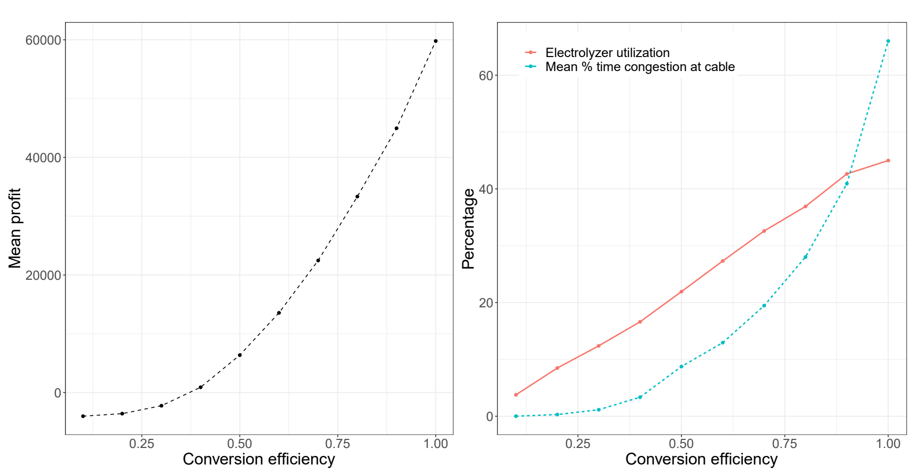

Fig. 12. Summary statistics and conversion efficiency (α).

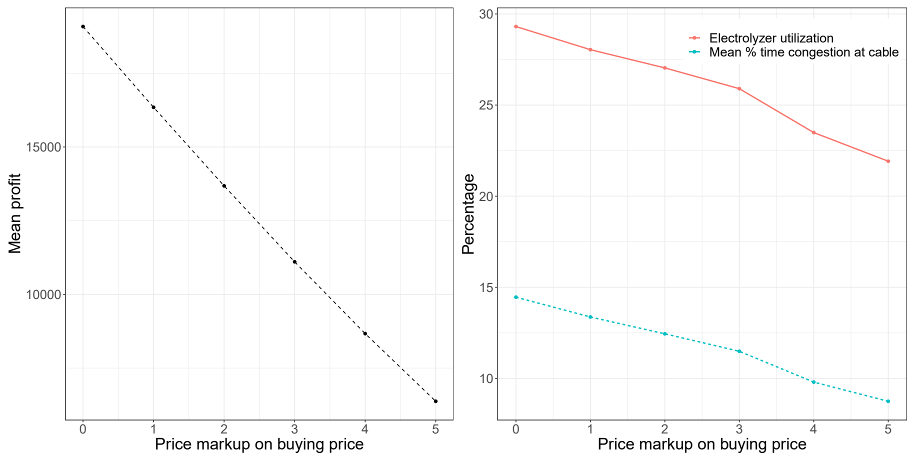

Fig. 13. Summary statistics and price markup on buying price (c^+).

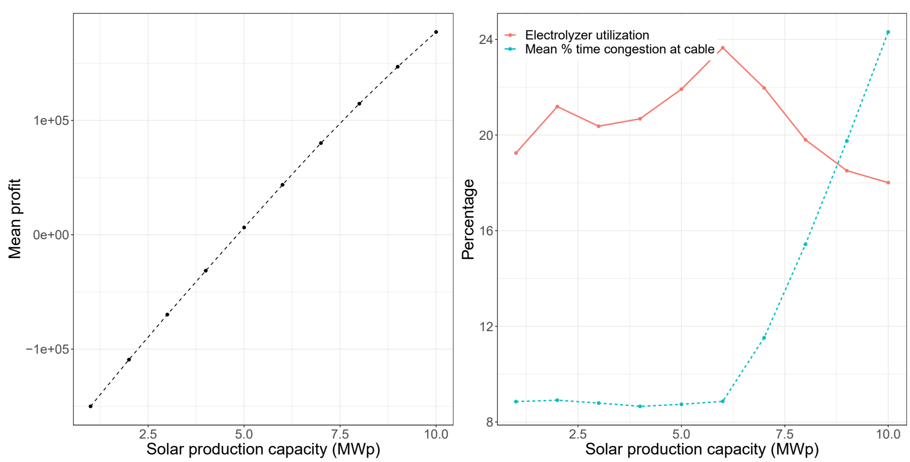

Fig. 14. Summary statistics and solar production capacity (w).

to increase linearly with increased production capacities. Up to 4 MWp of the conducted experiments, profits are negative, due to a high reliance on the grid to cover shortages and the inability to store energy when prices are low to cover future shortages. Increased reliance on the grid at low production capacities is reflected in the electrolyzer utilization rates, which increase for solar energy production capacities between 3 and 6 MWp and decrease for higher capacities. At low production capacities (e.g., $w = 1$), the electrolyzer is deployed to store energy that is bought from the grid to cover future shortages. Congestion at the connected cable increases nearly linearly for production capacities above 6 MWp. This is attributed to increased overages which are sold to the grid during summer. This highlights the importance of avoiding the installation of excess solar park capacity.

7. Conclusion

Increased decentralization of renewable energy sources such as solar parks leads to grid congestion in rural areas where grid distribution capacity is limited. At the same time, supplying local villages in the vicinity of solar parks reduces the need for long-distance energy transportation through the electricity grid. To reduce congestion and supply electricity to a local demand of households, hydrogen storage can be an important flexibility option to bridge the seasonality gap associated with supply and a local electricity demand when external distribution capacity is limited.

In this paper, we examine the problem of the owner of a solar park with local hydrogen storage who needs to decide how much to store, sell to or buy from an external electricity grid throughout the year and can supply energy to local electricity demand by households. Furthermore, the solar energy production and local electricity demand are seasonal and there is uncertainty associated with solar electricity supply, electricity demand, and variable electricity prices in the external electricity market. We propose a Markov decision process formulation to the above problem to optimize the expected profits per year from the perspective of the facility owner. We detail the optimal policies with regard to the period in which the actions take place (e.g., summer or winter). Moreover, we illustrate which actions are taken during overages and shortages throughout the year. We show how congestion levels for the grid operator and electrolyzer utilization are affected by conversion efficiency and strategic decisions such as the distribution capacity, storage capacity, and production capacity.

It is found that optimal policies are characterized by price thresholds that separate different types of actions. These include buying the maximum possible quantity, selling exactly overages or buying exact shortages, storing overages or obtaining shortages from storage, or selling the maximum amount possible. When distribution capacity is unconstrained, storage is not used for large periods of time. When distribution capacity is constrained, local congestion at the cable to which the solar park is connected is mostly caused by buying-related actions in winter, which are needed to cover potential future shortages. Under these conditions, increasing the level of storage capacity does not reduce congestion levels, because buying actions in winter remain necessary to cover shortages. For higher levels of distribution capacity, local congestion is mostly caused by selling-related actions of the overages in the summer. Counter-intuitively, local congestion increases for increased levels of storage capacity, because this enables increasing buying-related actions to prevent future shortages and exploiting price differences.

Mean profits are highly sensitive to the level of electrolyzer capacity and appear to increase linearly with capacity. Moreover, a lower electrolyzer utilization as a result of a large capacity is associated with higher profits than a low electrolyzer capacity with a higher utilization rate as a result of interacting with the electricity grid. This indicates that a high utilization rate of the electrolyzer is not necessarily an indication of increased profits. Hydrogen storage used to supply electricity does not lead to profits when distribution capacity is too small. Moreover, storage also does not aid in reducing local congestion at the connected cable when the associated distribution capacity is too small. This is because buying actions to prevent future shortages and benefit from price differences cause buying-related congestion at the cable connection. These actions are not aimed at reducing congestion, but at maximizing profits. Higher production capacities are associated with higher profits, even though this also causes higher congestion levels due to increased selling to the grid at times of abundant supply or high prices.

While a limited level of storage capacity is needed to cover shortages and overages when the distribution capacity is insufficient to handle peak loads of the solar park, a high level of storage capacity leads to increased local congestion problems for the grid operator when the SPH facility owner maximizes profits. Accordingly, the role of profit-oriented storage for solar parks as a source of flexibility to mitigate local congestion is limited, and a grid operator may need to expand distribution capacity to deal with this. Hence, we advise the grid operator to 1) establish price markups on sold electricity, 2) setting limits on the capacity of the solar park, 3) increase distribution capacity to alleviate local congestion problems.

The opportunities for future research are numerous and can be divided into two areas. The first area is centered around extending the model that we present in this work. For instance, new concepts arise in which local demand not only consists of electricity but also of hydrogen and, for example, demand for heat. Additionally, one could investigate the potential correlation between production and demand, or physical properties of using hydrogen as an energy carrier. Other future approaches may be focused on minimizing congestion instead of maximizing the storage owner's profits.

The other avenue for further research is the transition towards more strategic models. For instance, one may investigate the impact of multiple renewable energy systems with co-located storage facilities in grid-congestion issues. It would be interesting to research how the location of renewable energy systems in a grid can be optimized, with the aim of minimizing grid congestion.

Declaration of competing interest

The authors declare that they have no known competing financial interests or personal relationships that could have appeared to influence the work reported in this paper.

Acknowledgements

This study was supported by The Netherlands Organisation for Scientific Research (NWO) with grant number 438-15-519. Declarations of interest: None.

References

[1] K. Alanne, S. Cao, Zero-energy hydrogen economy (ZEH2E) for buildings and communities including personal mobility, Renew. Sustain. Energy Rev. 71 (2017) 697–711.
[2] S. Arora, J.W. Taylor, Forecasting electricity smart meter data using conditional kernel density estimation, Omega 59 (2016) 47–59.
[3] S. Babrowski, P. Jochem, W. Fichtner, Electricity storage systems in the future German energy sector: an optimization of the German electricity generation system until 2040 considering grid restrictions, Comput. Oper. Res. 66 (2016) 228–240.
[4] J.L. Bernal-Agustín, R. Dufo-López, Techno-economical optimization of the production of hydrogen from pv-wind systems connected to the electrical grid, Renew. Energy 35 (4) (2010) 747–758.
[5] U. Bünger, J. Michalski, F. Crotogino, O. Kruck, 7 - large-scale underground storage of hydrogen for the grid integration of renewable energy and other applications, in: M. Ball, A. Basile, T.N. Veziroğlu (Eds.), Compendium of Hydrogen Energy. Woodhead Publishing Series in Energy, Woodhead Publishing, Oxford, 2016, pp. 133–163.
[6] J. Boland, Characterising seasonality of solar radiation and solar farm output, Energies 13 (2) (2020) 471.
[7] E. Byon, Y. Ding, Season-dependent condition-based maintenance for a wind turbine using a partially observed markov decision process, IEEE Trans. Power Syst. 25 (4) (2010) 1823–1834.
[8] CBS, Returns, Co2 Emissions Electricity Production, 2020. URL, https://www.cbs.nl/nl-nl/maatwerk/2022/05/rendementen-co2-emissie-elektriciteit-sproductie-2020.
[9] A. Cretì, F. Fontini, Economics of Electricity: Markets, Competition and Rules, Cambridge University Press, 2019.
[10] M. Densing, Dispatch planning using newsvendor dual problems and occupation times: application to hydropower, Eur. J. Oper. Res. 228 (2) (2013) 321–330.
[11] R. Dufo-López, Optimisation of size and control of grid-connected storage under real time electricity pricing conditions, Appl. Energy 140 (2015) 395–408.
[12] ENTSOE, Transparency Platform, 2019. URL, https://transparency.entsoe.eu/transmission-domain/r2/dayAheadPrices/show.
[13] F.Y. Ettoumi, A. Mefti, A. Adane, M. Bouroubi, Statistical analysis of solar measurements in Algeria using beta distributions, Renew. Energy 26 (1) (2002) 47–67.
[14] Eurostat, Renewable Energy Statistics, 2020. URL, https://ec.europa.eu/eurostat/statistics-explained/index.php/Renewable_energy_statistics.
[15] E. Fertig, J. Apt, Economics of compressed air energy storage to integrate wind power: a case study in ERCOT, Energy Pol. 39 (5) (2011) 2330–2342.
[16] Flaticon, Icons Made by Freepik and Itim2101 from, 2020. URL, www.flaticon.com, www.flaticon.com.
[17] J. Gönsch, M. Hassler, Sell or store? An ADP approach to marketing renewable energy, OR spectrum 38 (3) (2016) 633–660.
[18] S. Grillo, A. Pievatolo, E. Tironi, Optimal storage scheduling using Markov decision processes, IEEE Trans. Sustain. Energy 7 (2) (2015) 755–764.
[19] L. Hannah, D.B. Dunson, Approximate dynamic programming for storage problems, in: ICML, 2011, pp. 337–344.
[20] M. Hassler, Heuristic decision rules for short-term trading of renewable energy with co-located energy storage, Comput. Oper. Res. 83 (2017) 199–213.
[21] R. Hemmati, H. Mehrjerdi, M. Bornapour, Hybrid hydrogen-battery storage to smooth solar energy volatility and energy arbitrage considering uncertain electrical-thermal loads, Renew. Energy 154 (2020) 1180–1187.
[22] IRENA, Green Hydrogen Cost 2020, 2020. URL, https://irena.org/-/media/Files/IRENA/Agency/Publication/2020/Dec/IRENA_Green_hydrogen_cost_2020.pdf.
[23] D.R. Jiang, W.B. Powell, An approximate dynamic programming algorithm for monotone value functions, Oper. Res. 63 (6) (2015) 1489–1511.
[24] D.R. Jiang, W.B. Powell, Optimal hour-ahead bidding in the real-time electricity market with battery storage using approximate dynamic programming, Inf. J. Comput. 27 (3) (2015) 525–543.
[25] J. Jorgenson, P. Denholm, T. Mai, Analyzing storage for wind integration in a transmission-constrained power system, Appl. Energy 228 (2018) 122–129.
[26] C. Keerthisinghe, A.C. Chapman, G. Verbič, PV and demand models for a Markov Decision Process formulation of the home energy management problem, IEEE Trans. Ind. Electron. 66 (2) (2019) 1424–1433.
[27] M. Korpås, C.J. Greiner, Opportunities for hydrogen production in connection with wind power in weak grids, Renew. Energy 33 (6) (2008) 1199–1208.
[28] G. Koudouris, P. Dimitriadis, T. Iliopoulou, N. Mamassis, D. Koutsoyiannis, Investigation on the stochastic nature of the solar radiation process, Energy Proc. 125 (2017) 398–404.
[29] A. Kumar, S. Srivastava, S. Singh, Congestion management in competitive power market: a bibliographical survey, Elec. Power Syst. Res. 76 (1) (2005)

153–164.
[30] P. Larscheid, L. Lück, A. Moser, Potential of new business models for grid integrated water electrolysis, Renew. Energy 125 (2018) 599–608.
[31] J. Lokar, P. Virtič, The potential for integration of hydrogen for complete energy self-sufficiency in residential buildings with photovoltaic and battery storage systems, Int. J. Hydrogen Energy 45 (60) (2020) 34566–34578.
[32] Y. Luo, Y. Shi, N. Cai, Chapter 3 - bridging a bi-directional connection between electricity and fuels in hybrid multienergy systems, in: Y. Luo, Y. Shi, N. Cai (Eds.), Hybrid Systems and Multi-Energy Networks for the Future Energy Internet, Academic Press, 2021, pp. 41–84.
[33] J. Märkle-Huß, S. Feuerriegel, D. Neumann, Cost minimization of large-scale infrastructure for electricity generation and transmission, Omega 96 (2020), 102071.
[34] N.B. Nederland, Basic Information about Energy Infrastructure, 2019. URL, https://www.netbeheernederland.nl/_upload/Files/Basisdocument_over_energie-infrastructuur_143.pdf.
[35] Nibud, Energy and Water, National Institute for Budget Education, 2019. URL, https://www.nibud.nl/consumenten/energie-en-water/.
[36] V. Papadopoulos, J. Desmet, J. Knockaert, C. Develder, Improving the utilization factor of a pem electrolyzer powered by a 15 mw pv park by combining wind power and battery storage – feasibility study, Int. J. Hydrogen Energy 43 (34) (2018) 16468–16478.
[37] G. Papaefthymiou, K. Dragoon, Towards 100% renewable energy systems: uncapping power system flexibility, Energy Pol. 92 (2016) 69–82.
[38] D. Pelzer, D. Ciechanowicz, A. Knoll, Energy arbitrage through smart scheduling of battery energy storage considering battery degradation and electricity price forecasts, in: 2016 IEEE Innovative Smart Grid Technologies - Asia (ISGT-Asia), 2016, pp. 472–477.
[39] M.L. Puterman, Markov Decision Processes: Discrete Stochastic Dynamic Programming, John Wiley & Sons, 2014.
[40] PVGIS, JRC Photovoltaic Geographical Information System (PVGIS) - European Commission, 2016. URL, https://re.jrc.ec.europa.eu/pvg_tools/en/tools.html#MR.
[41] M. Rouholamini, M. Mohammadian, Heuristic-based power management of a grid-connected hybrid energy system combined with hydrogen storage, Renew. Energy 96 (2016) 354–365.
[42] J. Shin, J.H. Lee, M.J. Realff, Operational planning and optimal sizing of microgrid considering multi-scale wind uncertainty, Appl. Energy 195 (2017) 616–633.
[43] I. Soares, M.J. Alves, C.H. Antunes, Designing time-of-use tariffs in electricity retail markets using a bi-level model – estimating bounds when the lower level problem cannot be exactly solved, Omega 93 (2020).
[44] T. Soubdhan, R. Emilion, R. Calif, Classification of daily solar radiation distributions using a mixture of dirichlet distributions, Sol. Energy 83 (7) (2009) 1056–1063.
[45] Statista, Lithium-ion Battery Pack Costs Worldwide between 2011 and 2030, 2020. URL, https://www.statista.com/statistics/883118/global-lithium-ion-battery-pack-costs/.
[46] B. Steffen, C. Weber, Optimal operation of pumped-hydro storage plants with continuous time-varying power prices, Eur. J. Oper. Res. 252 (1) (2016) 308–321.
[47] L.S. Vargas, G. Bustos-Turu, F. Larraín, Wind power curtailment and energy storage in transmission congestion management considering power plants ramp rates, IEEE Trans. Power Syst. 30 (5) (2014) 2498–2506.
[48] A.T. Veenstra, A.H. Schrotenboer, M.A.J. Uit het Broek, E. Ursavas, Green Hydrogen Plant: Optimal Control Strategies for Integrated Hydrogen Storage and Power Generation with Wind Energy, 2021.
[49] T. Wang, S. Deng, Multi-period energy procurement policies for smart-grid communities with deferrable demand and supplementary uncertain power supplies, Omega 89 (2019) 212–226.
[50] Y. Wang, Y. Dvorkin, R. Fernández-Blanco, B. Xu, D.S. Kirschen, Impact of local transmission congestion on energy storage arbitrage opportunities, in: 2017 IEEE Power & Energy Society General Meeting, IEEE, 2017, pp. 1–5.
[51] T. Weitzel, C.H. Glock, Energy management for stationary electric energy storage systems: a systematic literature review, Eur. J. Oper. Res. 264 (2) (2018) 582–606.
[52] C.-K. Woo, I. Horowitz, A. Olson, B. Horii, C. Baskette, Efficient frontiers for electricity procurement by an LDC with multiple purchase options, Omega 34 (1) (2006) 70–80.
[53] Øystein Ulleberg, R. Hancke, Techno-economic calculations of small-scale hydrogen supply systems for zero emission transport in Norway, Int. J. Hydrogen Energy 45 (2) (2020) 1201–1211, international Hydrogen and Fuel Cell Conference 2018, Trondheim, Norway.
[54] A. Zakaria, F.B. Ismail, M.H. Lipu, M. Hannan, Uncertainty models for stochastic optimization in renewable energy applications, Renew. Energy 145 (2020) 1543–1571.
[55] Y. Zhang, P.E. Campana, A. Lundblad, J. Yan, Comparative study of hydrogen storage and battery storage in grid connected photovoltaic system: storage sizing and rule-based operation, Appl. Energy 201 (2017) 397–411.
[56] Y.H. Zhou, A. Scheller-Wolf, N. Secomandi, S. Smith, Managing wind-based electricity generation in ;the presence of storage and transmission capacity, Prod. Oper. Manag. 28 (4) (2019) 970–989.